The effect of post-deposition annealing on the optical properties of filtered vacuum arc deposited ZnO–SnO_2

2007 J. Phys.: Condens. Matter 19 256206

(http://iopscience.iop.org/0953-8984/19/25/256206)

IOP PUBLISHING JOURNAL OF PHYSICS: CONDENSED MATTER

J. Phys.: Condens. Matter **19** (2007) 256206 (10pp) doi:10.1088/0953-8984/19/25/256206

The effect of post-deposition annealing on the optical properties of filtered vacuum arc deposited ZnO–SnO_2

E Çetinörgü[1,2,5], **S Goldsmith**[1,3] **and R L Boxman**[1,4]

[1] Electrical Discharge and Plasma Laboratory, Tel Aviv University, POB 39040, Tel Aviv 69978, Israel
[2] Physics Department, Çukurova University, 01330 Adana, Turkey
[3] Sackler Faculty of Exact Sciences, School of Physics and Astronomy, Tel Aviv University, POB 39040, Tel Aviv 69978, Israel
[4] Fleischman Faculty of Engineering, Tel Aviv University, POB 39040, Tel Aviv 69978, Israel

E-mail: eda@eng.tau.ac.il (E Çetinörgü)

Received 18 November 2006, in final form 19 April 2007
Published 5 June 2007
Online at stacks.iop.org/JPhysCM/19/256206

Abstract

Zinc stannate (ZnO–SnO_2) thin films were deposited on ultraviolet fused silica (UVFS) substrates using filtered vacuum arc deposition (FVAD). During deposition, the substrates were at 200 and 400 °C. As-deposited films were annealed at 500 and 600 °C in Ar for 50 min. The structure was determined before and after annealing using x-ray diffraction (XRD). The XRD patterns of all ZnO–SnO_2 thin films had an amorphous structure. The average optical transmission of the film in the visible spectrum was >80% and was affected by annealing. The films' optical constants in the 250–989 nm wavelength range were determined by variable angle spectroscopic ellipsometry (VASE). The refractive indexes of as-deposited and annealed films were in the ranges 1.95–2.35 and 2.0–2.32, respectively. The extinction coefficients of as-deposited annealed films were in the same range, approximately 0–0.5. However, in the UV range (<450 nm) the extinction coefficient values decreased significantly for annealed films. The optical energy band gap (E_g) was determined by the dependence of the absorption coefficient on the photon energy at short wavelengths. It varied between 3.65 and 3.72 eV for annealed films as a function of deposition pressure. Although the lowest electrical resistivity of zinc stannate films obtained for as-deposited films on 400 °C heated substrates, using 0.93 Pa oxygen pressure, was 1.08×10^{-2} Ω cm, highly resistive films (>10^5 Ω cm) were obtained by annealing.

[5] Author to whom any correspondence should be addressed.

1. Introduction

Transparent conducting oxide (TCO) films such as In_2O_3, SnO_2, and ZnO with dopants like Al, Sb etc are widely used in optoelectronic devices due to their attractive properties [1]. The growing demand for improved performance and low-cost optoelectronic devices has resulted in an effort to develop new alternative TCO materials to replace the commercial ones, and recently various multi-component TCO thin films have been reported [2, 3]. These new TCOs include binary and multi-component metal oxides of Zn, Cd, Sn and In with various dopands [4, 5]. ZnO–SnO_2, in thin film form, has emerged as a promising candidate for optoelectronic devices and gas sensors due to its large optical band gap ($E_g \sim 3.6$ eV [6, 7]), resulting in high transmittance from the UV to the infrared regime, and its conductivity could be as low as 10^{-3} Ω cm, depending on the deposition conditions. The ZnO–SnO_2 thin films have been deposited using vacuum arc plasma evaporation [8], pulsed laser deposition [9], magnetron sputtering [10–13] and filtered vacuum arc deposition (FVAD) [14, 15].

The aim of the work is to deposit highly transparent and conducting ZnO–SnO_2 films using a FVAD system, and to investigate the following effects: post-deposition annealing on the structure; the optical and electrical properties, in particular looking on the one hand for improved transmittance and conductivity, and on the other hand on the interdependence of the film structure and their characteristics. Structure analysis was performed by XRD, and the detailed optical characterization of the films was performed using normal incidence transmission and *ex situ* variable angle spectroscopic ellipsometry (VASE), and the electrical resistivity was obtained using four-point probe data.

2. Film preparation and characterization

Cylindrical Zn–Sn cathodes (90 mm diameter) were prepared from 50 at.% Zn and 50 at.% Sn, 99.99% pure metals, and they were used to deposit the ZnO–SnO_2 thin films by FVAD system. The deposition system has been described previously by Ben-Shalom *et al* [16] and Kaplan *et al* [17]. In the present work the substrates were placed 15 cm further away from the macroparticle filter exit. The thin films were deposited using a 150 A arc current and a 60 s deposition time on 200 and 400 °C heated substrates. The oxygen background pressure was varied in steps of 0.13 Pa between deposition runs in the range 0.53–1.06 Pa, for 400 °C heated substrates, and was 0.93 Pa for 200 °C heated substrates. The substrates used were $76 \times 25 \times 1$ mm commercial microscope glass slides and $50 \times 50 \times 1$ mm UV fused silica (UVFS). The deposited films were annealed at 500 and 600 °C in Ar for 50 min in total with 5 min heating time, 30 min annealing, and 15 min cooling time. The annealing temperature was kept below 600 °C so that the samples would not be damaged, and 500 °C was chosen, in order to have a comparative data base with the literature.

The structural analyses were performed using a Scintag x-ray diffractometer with Cu Kα radiation (wavelength $\lambda = 1.541$ Å). Optical measurements of all films were performed using an ultraviolet–visible–near-infrared (UV–VIS–NIR) double-beam spectrophotometer (JASCO V-530) in the wavelength range of 250–1100 nm relative to air, and a variable angle spectroscopic ellipsometer (J A Woollam M-2000). A detailed description of the measured ellipsometric parameters (measured with an accuracy of $\pm 0.01°$), the fitting procedure for the measured and the calculated data, and the optical models that were used have been described previously [18, 19]. Measurements were taken in the wavelengths range 250–989 nm at three angles of incidence, 60°, 65° and 70°, to yield adequate sensitivity over the full spectral range. The absorption coefficient, $\alpha(\lambda)(= 4\pi k(\lambda)/\lambda)$, was calculated from the $k(\lambda)$ values determined from spectroscopic ellipsometry. When the valance and conduction bands densities

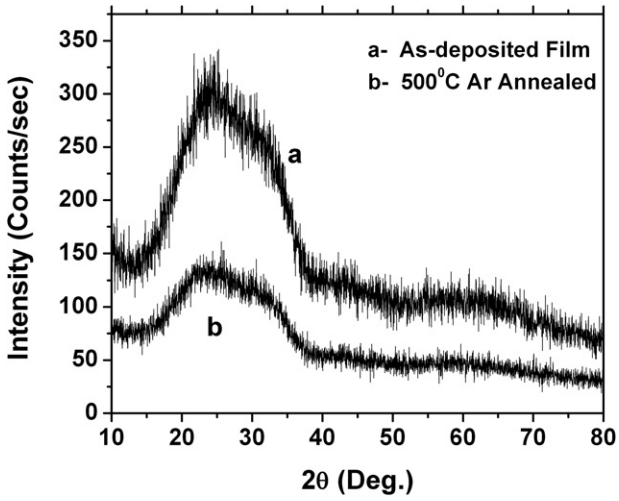

Figure 1. XRD patterns of as-deposited and 500 °C annealed ZnO–SnO_2 thin films.

of states are parabolic, the absorption coefficient α for $E > E_g$ is given by the expression:

$$\alpha(E) = B\frac{(E - E_g)^m}{E} \tag{1}$$

where E is the photon energy, E_g is the optical band gap and m is a power factor, which is generally $1/2$ for direct band gap materials [20]. Assuming that $m = 1/2$, the optical energy band gap is defined by extrapolating the linear part of the absorption spectrum to 0.

The electrical resistivity of the film was determined for as-deposited and annealed films as a function of the deposition pressure using the four-probe method. All film characterization and diagnostics were performed at the centre of the deposited film, over an area of $\sim 1 \times 1$ cm, where the thickness non-uniformity was within $\sim 5\%$.

3. Results

3.1. XRD analysis

In figure 1, typical XRD diffraction patterns of as-deposited ZnO–SnO_2 thin films deposited on 400 °C heated substrate ata pressure of 0.93 Pa and annealed at 500 °C in Ar are presented. The amorphous broad band between 25° and 35° is associated with the glass substrate. All as-deposited films were amorphous, independent of the deposition pressure and substrate temperature. As can be seen in figure 1, the structure of films was not changed by annealing at 500 °C in Ar. Furthermore, the films annealed at 600 °C contained many cracks, preventing structure analyses.

3.2. Optical and electrical analyses

Typical plots of transmission spectra of ZnO–SnO_2 samples deposited on 200 °C heated substrate at a pressure of 0.93 Pa and annealed at 500 °C in Ar are presented in figure 2. As can be seen, the transmission edge shifted to shorter wavelengths (or to higher photon energy) after annealing in Ar, compared to the transmission of the same films. The average transmission in the visible spectrum for all deposited and annealed films was 80–85% (measured with an

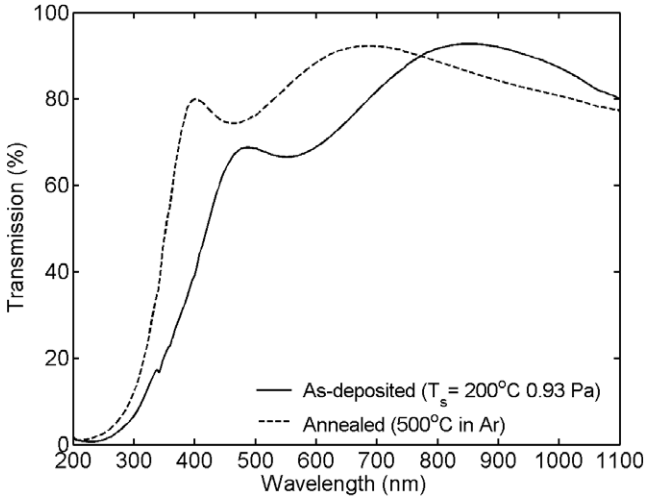

Figure 2. Optical transmission plots of as-deposited (at 200 °C) and annealed ZnO–SnO_2 thin films.

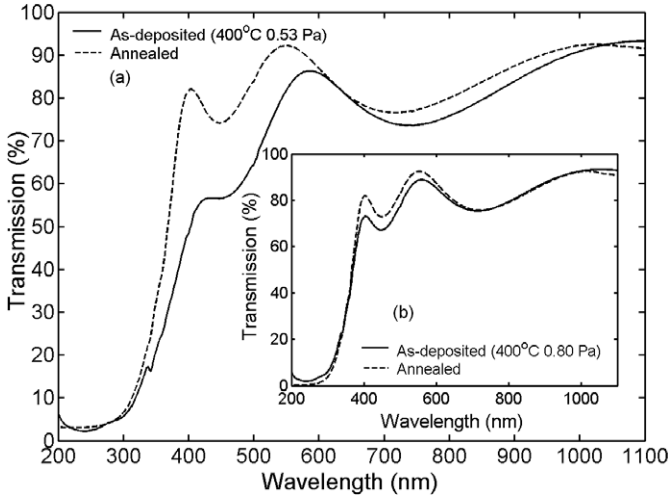

Figure 3. Optical transmission plots of (a) as-deposited and (b) annealed ZnO–SnO_2 thin films as a function of deposition pressure.

accuracy of ±0.1%). Furthermore, as-deposited films at a lower deposition pressure (<0.80 Pa) had a brownish colour that disappeared after annealing in Ar atmosphere.

In figures 3(a) and (b), the optical transmission of ZnO–SnO_2 thin films deposited on UVFS substrates at 400 °C with a pressure of 0.53 Pa, and a pressure of 0.80 Pa and annealed at 500 °C for 50 min in Ar are presented, respectively. As can be seen from figure 3(a), the optical band edge shifted to lower wavelengths after annealing; however, this shift was weaker for films deposited at higher deposition pressures (figure 3(b)). The highest transmission in the visible was in the range 80–85%, and was not affected by the deposition pressure and deposition temperature. Optical transmission in the UV spectral range improved significantly independently of the deposition temperature at lower deposition pressures (<0.80 Pa).

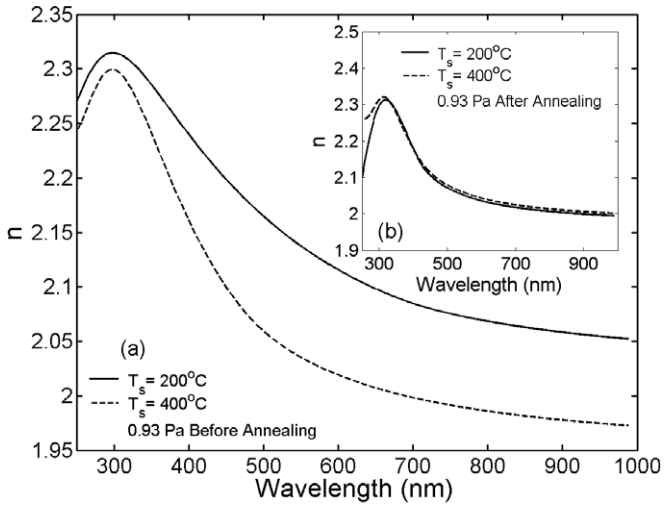

Figure 4. Plots of the refractive index of (a) as-deposited and (b) annealed ZnO–SnO_2 thin films versus wavelength as a function of substrate temperature.

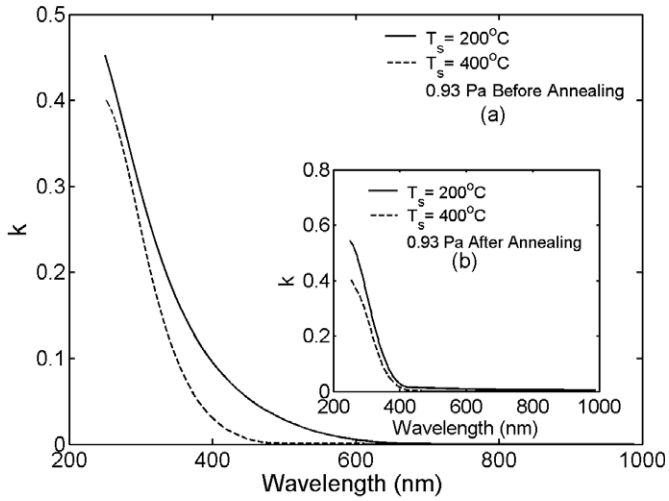

Figure 5. Plots of the extinction coefficient of (a) as-deposited and (b) annealed ZnO–SnO_2 thin films versus wavelength as a function of substrate temperature.

In figures 4(a) and (b), typical plots of the refractive indexes of films deposited on 200 and 400 °C heated substrates at a pressure of 0.93 Pa and annealed at 500 °C are presented, respectively. The refractive index of as-deposited films decreased with increasing wavelength from approximately 2.3 to 1.98 and, after annealing, from 2.3 to 2.0. Furthermore, the difference between the refractive index values of films deposited on 200 and 400 °C heated substrates decreased with the annealing (figure 4(b)), converging to the same n values independently of the deposition pressure. In figures 5(a) and (b), the dependence on wavelength and annealing temperature is shown for the extinction coefficients. The k values of films deposited on 200 and 400 °C heated substrates decreased from 0.5 at 250 nm to approximately 0.05 and 0.1 at 400 nm, and then to zero at longer wavelengths, respectively. Increasing the

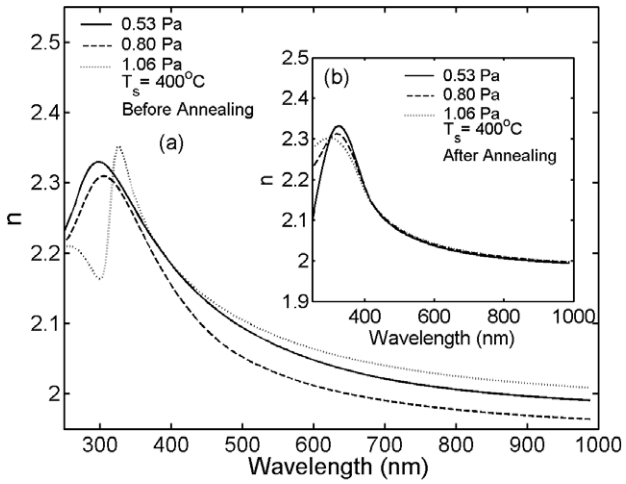

Figure 6. Plots of the refractive index of (a) as-deposited and (b) annealed ZnO–SnO_2 thin films versus wavelength as a function of deposition pressure.

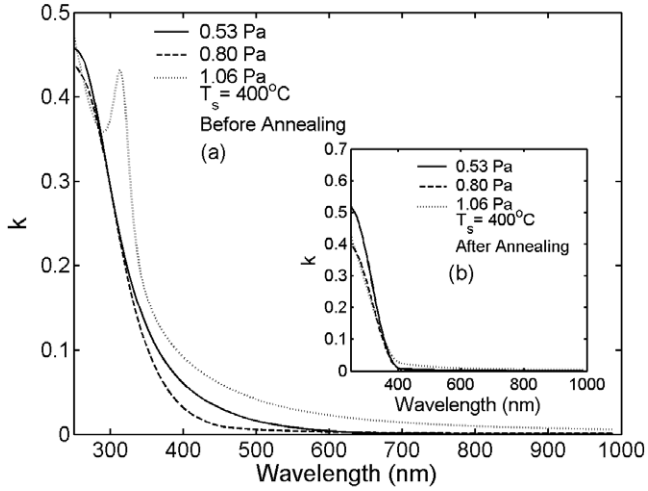

Figure 7. Plots of the extinction coefficient of (a) as-deposited and (b) annealed ZnO–SnO_2 thin films versus wavelength as a function of deposition pressure.

substrate temperature of as-deposited films decreased the extinction coefficients (figure 5(a)). The decrease in k seen below 450 nm for annealed samples is very sharp, where a significant change in k was observed for annealed films (figure 5(b)). The effects of annealing on the optical constants of films that were deposited at pressures of 0.53, 0.80 and 1.06 Pa are presented in figures 6(a) and (b). As previously presented by us, no correlation was found between the deposition pressure and the values of refractive index [19]. As is seen from figure 6(b), in the visible spectrum the values of the refractive index of annealed films are approximately the same, independently of deposition pressure. In figures 7(a) and (b), the extinction coefficients of the same films before and after annealing are presented. Similarly, the k values decreased with increasing wavelength and showed lower values in the UV region compared to the k of as-deposited films.

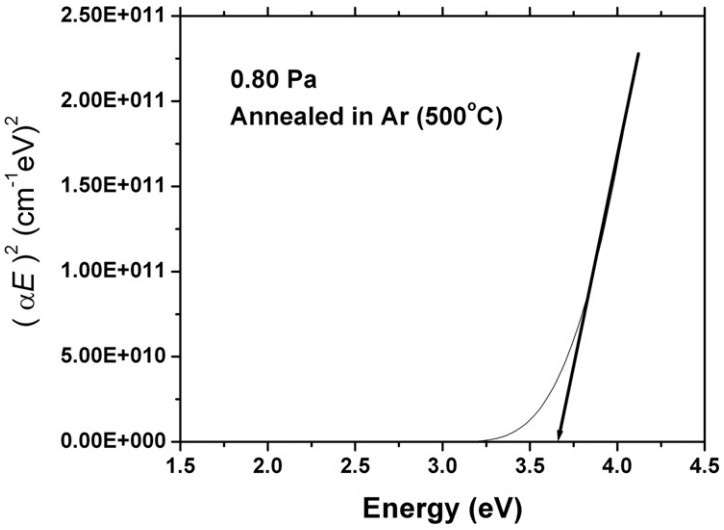

Figure 8. Plot of $(\alpha E)^2$ versus E.

Table 1. Optical constants, n and k, at 550 nm, and the optical band gap E_g for as-deposited and annealed ZnO–SnO_2 thin films.

	As-deposited			Annealed		
Pressure (Pa)	n	k	E_g (eV)	n	k	E_g (eV)
0.53	2.07	0.010	3.61	2.05	0.002	3.65
0.67	2.06	0.010	3.64	2.05	0.002	3.66
0.80	2.03	0.004	3.70	2.05	0.001	3.69
0.93	2.04	0.001	3.68	2.06	0.0003	3.68
1.06	2.08	0.030	3.69	2.06	0.010	3.70
0.93[a]	2.14	0.013	3.53	2.05	0.01	3.65

[a] Annealing in Ar for 30 min /Films deposited on 200 °C and 400 °C heated substrates.

In table 1, the refractive index and the extinction coefficients at 550 nm and the optical energy band gap values for as-deposited and annealed ZnO–SnO_2 thin films are presented. The accuracy of the optical constants is 0.25%, and the accuracy of E_g is ± 0.01 eV. The values of n for films deposited on 400 °C heated substrates with pressures in the range 0.53–1.06 Pa were 2.03–2.08, and were $\sim$2.05 after annealing, independently of deposition pressure. The index of refraction of films deposited on 200 °C heated substrates also changed after annealing, being 2.14 before annealing and 2.05 after annealing. The values of k were in the range of approximately 0–0.03 for both as-deposited and annealed films. The values of k were only changed significantly at shorter wavelength regions, where $\lambda < 450$ nm. In figure 8, a plot of $(\alpha E)^2$ versus E of ZnO–SnO_2 film deposited at 0.80 Pa and annealed at 500 °C is presented as an example, where the straight line portion of the absorption spectrum is extrapolated to $(\alpha E)^2 = 0$ in order to determine the value of E_g. As can be seen in table 1, the derived E_g values for as-deposited films are in the range 3.53–3.69 eV [19], and 3.65–3.72 eV for annealed films. The most significant change in E_g was observed for films deposited at 0.53 Pa oxygen pressure with annealing, as can also be seen from optical transmission measurements.

The electrical resistivities of ZnO–SnO_2 thin films were calculated using the data obtained by the four-point probe method. The sheet resistance R (Ω/square) and the resistivity of

the films were determined previously as a function of the deposition pressure and substrate temperature [19]. The films deposited at a pressure $\geqslant$0.8 Pa on 200 °C heated substrates had a resistivity in the range 2.18×10^{1}–4.34×10^{2} Ω cm, decreasing with the pressure. However, the films deposited on substrates at 400 °C with a deposition pressure in the range 0.53–1.06 Pa were conducting, where the films deposited at 0.93 Pa had the lowest resistivity $\sim 1.08 \times 10^{-2}$ Ω cm. In addition, with decreasing pressure and temperature, the film's conductivity also decreased. In contrast, the resistivity of films annealed in Ar at 500 °C increased significantly ($>10^{5}$ Ω cm) and was independent of substrate temperature and the deposition pressure.

4. Discussion

The objective of this work was to characterize ZnO–SnO_2 thin films deposited using an FVAD system, studying the effects of the deposition parameters and post-deposition annealing on the film properties.

4.1. Film structure

FVA deposited films that were on 200 and 400 °C substrates and later annealed in Ar at 500 °C for 50 min were amorphous, independently of the deposition pressure. The structure of zinc stannate reported in the literature is mostly amorphous, depending on the composition, annealing temperature and substrate temperature [9–11, 13]. Perkins *et al* [9] reported on the crystalline structure of (111) orientation ZnO–SnO_2 thin films annealed in vacuum at 700 °C. A similar observation was made by Minami *et al* [11] who found that ZnO–SnO_2 films deposited at 300 °C were amorphous when the Zn atomic concentration ratio was in the range 20–80%. Satoh *et al* [12] investigated crystalline films with (111) preferred orientation after post-deposition annealing at 750 °C in air, whereas as-deposited films had no sharp x-ray diffraction peaks. Previously, we also obtained amorphous ZnO–SnO_2 thin films deposited at room temperature (RT) using different arc currents and annealed at 500 °C in air [15]. As we see from our results, the main advantage of annealing, even without having crystalline material, is to improve the UV transmittance, as discussed in the next section.

4.2. Optical and electrical properties

The optical transmission of the films in the visible spectral region is in the range 80%–85%, similar to that reported previously by Minami *et al* [21]. After annealing, the transmittance edge of ZnO–SnO_2 films in the UV region shifted to lower wavelengths and has a sharp decrease in this region, indicating a well-defined and a wider optical band gap. Defects in crystals and in disordered materials could have an effect on the materials' structure and electronic properties. Moreover, the effect on the optical properties can be seen from transmission plots where the defects and disorder can be examined by observing the change in band tailing. As mentioned above, the optical band edge shifts with annealing and on using heated substrates. The most significant effect on the UV transmission by annealing and by using heated substrates is due to their effect on the band tailing (by defects and impurities), and not necessarily by crystallization. This was observed by us when the films remain amorphous after annealing. Furthermore, the observed significant change in the films' optical band edge with annealing, when they are deposited at lower pressures, also indicates that the deposited films have weak optical quality compared to high-pressure-deposited films, since the band tailing is stronger in films deposited at a low deposition pressure (<0.80 Pa).

In the present work, the optical parameters and their dependence on the deposition conditions are derived from ellipsometry data, and are found to depend on the deposition conditions. Hence, the data shown in figures 4–7 actually reflect the overall dependence of the optical parameters and thickness on post-deposition annealing. The optical parameters, n and k, of the films that are reported here do not differ significantly from those reported by Young *et al* [7] and Satoh *et al* [12] for as-deposited and annealed ZnO–SnO_2 thin films. The optical constants n and k decreased with wavelength, and at 550 nm [7] and 600 nm [12] were approximately 2 and 0. The variations in the films' optical parameters could also be affected by the stress induced in the films during the annealing that produces a change in defect structure. It should be also noted that, as can be seen from figures 4 and 6, the peak of the refractive index values did not significantly shift to the shorter wavelengths with annealing, and does not correlate with the shifting of the optical band edge in the films. The decrease in k values in the shorter-wavelength region after annealing improved the transparency in the UV region. Such a decrease of k indicates weaker photon absorption by electron transitions across the band gap, where fewer intermediate defect levels could be present after the annealing. We believe that the change in the amount of disorder, and hence the defect structure, resulted in a change in optical parameters. The increase in E_g could be due to an improvement in the film structure as it becomes more ordered, which affects the band gap broadening by a decrease in band gap defects.

In previous research [19], we reported the effect of the substrate temperature on the film characteristics, where the films deposited at 400 °C showed the lowest resistivity, whereas the others were non-conducting. The resistivity of these films decreased when the pressure increased from 0.53 to 0.93 Pa, and then increased with further increase in the pressure. However, post-deposition annealing in Ar at 500 °C produced non-conducting films with a resistivity $>10^5$ Ω cm, independently of the deposition conditions. In [12], Satoh *et al* studied the effect of the Ar/O_2 flow ratio on the film's resistivity and post-deposition annealing. The films deposited with an Ar/O_2 mixture had $\sim 10^5$ Ω cm resistivity, whereas, the films deposited in pure Ar had on the order of 10^{-2} Ω cm. In addition, since the post-deposition annealing yielded a number of cracks, the electrical properties could not be investigated. This was attributed to the thermal expansion coefficients of the substrate and the film. We also could not measure the resistivity of films annealed at 600 °C in Ar at all deposition conditions, e.g. pressure and substrate temperature, since many cracks were produced during the post-deposition annealing process. This also affected the optical and structure measurements.

5. Conclusions

The amorphous phase was observed for ZnO–SnO_2 thin films deposited on 200 and 400 °C heated substrates. Annealing at 500 °C in Ar atmosphere did not affect the structure of films deposited at different substrate temperatures and deposition pressures. As-deposited films had a maximum transmission of about 80–85%; annealing improved the average transmission in the UV spectral region ∼10%. The direct optical band gap was increased to a wider band gap, from 3.61–3.70 eV to 3.65–3.72 eV with annealing, indicating a better-arranged band gap. The most significant change was in the optical gap for films deposited at lower deposition pressures. The value of the refractive index at 550 nm was mostly constant for annealed films (∼2.05), independently of the deposition pressure. In addition, the k values decreased with annealing for a shorter wavelength region, where it was approximately zero at >400 nm wavelength. Although, annealing at 500 °C improved optical transmission in the UV, it had a detrimental effect on the electrical conductivity. In addition, annealing at higher temperatures (⩾600 °C) damaged all FVA-deposited ZnO–SnO_2 films, preventing measurements.

Acknowledgments

E Çetinörgü is grateful for a scholarship offered by the Israeli Government to foreign students. The authors thank Dr Rosenberg for the XRD measurements.

References

[1] Minami T 2005 *Semicond. Sci. Technol.* **20** S35–44
[2] Coutts T J, Perkins J D, Ginley D S and Mason T O 1999 *Proc. 195th Meeting of the Electrochemical Society (Seattle, WA)* NREL/CP 520-26640
[3] Minami T 2000 *MRS Bull.* **25** 38
[4] Ginley D S and Bright C 2000 *MRS Bull.* **25** 15
[5] Wu X, Coutts T J and Mulligan W P 1997 *J. Vac. Sci. Technol.* A **15** 1057
[6] Coutts T J, Young D L and Li X 2000 *J. Vac. Sci. Technol.* A **18** 2646
[7] Young D L, Moutinho H, Yan Y and Coutts T J 2002 *J. Appl. Phys.* **92** 310
[8] Minami T, Tsukada S, Minamino Y and Miyata T 2005 *J. Vac. Sci. Technol.* A **23** 1128
[9] Perkins J D, Del Cueto J A, Allenman J L, Warmsingh C, Keyes B M, Gedvilas L M, Parilla P A, To B, Readey D W and Ginley D S 2002 *Thin Solid Films* **411** 152
[10] Moriga T, Hayashi Y, Kondo K, Nishimura Y and Murai K 2004 *J. Vac. Sci. Technol.* A **22** 1705
[11] Minami T, Sonohara H, Takata S and Sato H 1994 *Japan. J. Appl. Phys.* **33** L1693
[12] Satoh K, Kakehi Y, Okamoto A and Murakami S 2005 *Japan. J. Appl. Phys.* **44** L34
[13] Young D L, Williamson D L and Coutts T J 2002 *J. Appl. Phys.* **91** 1464
[14] Çetinörgü E, Goldsmith S and Boxman R L 2006 *J. Appl. Phys.* D **39** 1878
[15] Çetinörgü E, Goldsmith S and Boxman R L 2006 *Semicond. Sci. Technol.* **21** 364–9
[16] Ben-Shalom A, Kaplan L, Boxman R L, Goldsmith S and Nathan M 1993 *Thin Solid Films* **236** 20
[17] Kaplan L, Zhitomirsky V N, Boxman R L, Goldsmith S and Rusman I 1995 *Surf. Coat. Technol.* **76/77** 181–9
[18] Çetinörgü E, Goldsmith S, Zhitomirsky V N, Boxman R L and Bungay C L 2006 *Semicond. Sci. Technol.* **21** 1303
[19] Çetinörgü E, Goldsmith S, Barkay Z and Boxman R L 2006 *J. Appl. Phys.* D **39** 5245
[20] Wooten F 1972 *Optical Properties of Solids* (New York: Academic)
[21] Minami T, Takata S, Sato H and Sonohara H 1995 *J. Vac. Sci. Technol.* A **13** 1095